The 9th European Congress on Computational Methods in Applied Sciences and Engineering
ECCOMAS Congress 2024
3–7 June 2024, Lisboa, Portugal

LEVERAGING QUADRILATERAL MESHES IN NEFEM FOR ENHANCED CAD-TO-ANALYSIS INTEGRATION

Gian Maria Santi[1], Mattia Montanari[2] AND Ruben Sevilla[3]

[1] Department of Industrial Engineering, University of Bologna, Italy,
gianmaria.santi2@unibo.it

[2] Huawei Munich Research Center, Munich, Germany and Oxford University, Oxford, UK

[3] Zienkiewicz Centre for Computational Engineering, Swansea University, UK

Key words: Computational Mechanics, NEFEM, FEM, Complex Geometry

Summary. The preparation of CAD geometries for meshing and analysis poses a significant challenge in engineering simulations due to its labor-intensive nature. Over the last 20 years, various methods have been proposed to bridge the gap between CAD and analysis by requesting CAD to produce volume represents (V-Rep) suitable for the analysis . However, these methods do not integrate with modern CAD software (which do not produce V-Reps) and have not found wide industrial applicability. Our study extends the capabilities of the NURBS Enhanced Finite Element Method (NEFEM), a CAD-friendly technique that offers distinct advantages. NEFEM combines boundary representation (B-Rep) from common CAD packages with volume representation (V-Rep) from established meshing tools, resulting in a super-parametric element formulation for direct analysis of the CAD geometry. Our research introduces high-order quadrilateral elements and presents a comparison with their finite element counterparts. Through established benchmarks, the study demonstrates geometric convergence and underscores a superior CAD interoperability of NEFEM that could not be achieved with other methods.

1 Introduction

The integration of geometric design and analysis in computational engineering represents a crucial challenge, particularly when using methods that ensure accurate geometric representation within the simulation process. The NURBS-enhanced finite element method (NEFEM) emerges as a promising technique in this context [1, 2, 3], offering the ability to directly incorporate the boundary representation (B-rep) provided by CAD systems without the need for conversion to a volumetric representation (V-rep) [4, 5, 6]. This approach not only reduces geometric errors associated with discretization but also enhances the accuracy of simulations across various application areas, including heat transfer, electromagnetism, and fluid dynamics. This work aims to investigate the effectiveness of NEFEM using elements with polynomial degree $p = 2$. The primary objective is to evaluate the advantages in terms of accuracy and convergence compared to standard formulations and lower-order NEFEM. Through a series of numerical examples, we will demonstrate how increasing the polynomial degree can expand the applicability of NEFEM, making it a competitive choice for complex problems in structural engineering, emerging lattice structure applications [7] and fluid dynamics.

2 Methodology

2.1 Background

The NURBS-enhanced finite element method (NEFEM) was developed to address the limitations of traditional finite element methods (FEM) in integrating with CAD systems. While standard FEM [8, 9] relies on an approximate polynomial representation of geometry, NEFEM leverages the exact boundary representation (B-rep) provided by CAD models. This approach allows for precise geometric descriptions, thereby improving the accuracy of simulations.

The primary difference between FEM, isogeometric analysis (IGA), and NEFEM lies in how they handle geometric representation. FEM uses a piecewise polynomial description, which can introduce geometric errors. IGA, on the other hand, employs NURBS to represent the entire volume but requires a complex transformation from B-rep to volumetric representation (V-rep). NEFEM takes a hybrid approach, directly using the CAD B-rep for boundary elements, thereby maintaining an exact match with the CAD geometry. Traditionally, NEFEM has been applied only to triangular or tetrahedral meshes, limiting its applicability in contexts where quadrilateral or hexahedral elements are preferred, such as in nonlinear solid mechanics.

Quadrilateral elements are highly significant in the field of structural simulation as they enable the generation of structured meshes, which are crucial for accurate and efficient analysis. Linear quadrilateral elements have been extensively studied in a previous paper from the authors [10]. This work presents an extension of NEFEM to quadrilateral elements with a polynomial degree $p = 2$.

The proposed approach introduces a new super-parametric mapping that preserves the exact boundary representation for quadrilateral elements in any field approximation. This mapping is based on NURBS curves defining the element edges, ensuring tight integration with CAD and enhancing simulation accuracy. For solving the weak form, numerical integration is performed using Gaussian quadratures adapted to the rational nature of NURBS curves, thereby reducing integration errors.

Several numerical examples demonstrate the effectiveness of this approach, showing significant error reduction compared to traditional finite elements. This formulation is particularly beneficial in structural mechanics and fluid dynamics problems, where geometric accuracy is crucial.

2.2 Mapping

For FEM elements the mapping from parent space $[0, 1]^2$ (derived from the most used parent space $[-1, 1]^2$) to physical element is the classical isoparametric mapping, given by Eq. 1.

$$\boldsymbol{\phi}(\xi, \eta) = \sum_{k=1}^{4} N_k(\xi, \eta)\, \boldsymbol{\phi}_k, \tag{1}$$

where N_k is the bi-linear shape function associated to node (ξ_k, η_k).

The mapping for NEFEM quadrilateral elements is a non isoparametric formulation that came from the Coons patch [11], an injective and continuously differentiable function able to parameterize the surface enclosed by four curves (Eq. 2).
This solution maps from the parent space $[0, 1]^2$ to a quadrilateral NEFEM element Ω_e as follow:

$$\boldsymbol{\phi}(\xi,\eta) = \underbrace{\sum_{i=1}^{2} \tilde{N}_i(\eta)\mathbf{C}_i(\xi) + \sum_{j=1}^{2} \tilde{N}_j(\xi)\mathbf{D}_j(\eta)}_{\text{A}} - \underbrace{\sum_{k=1}^{4} N_k(\xi,\eta)\mathbf{x}_k}_{\text{B}}, \tag{2}$$

where $\{\tilde{N}_l\}_{l=1,2}$ denote the linear shape functions in the one-dimensional reference element $[0,\ 1]$. The parametric curves $\{\mathbf{C}_l\}_{l=1,2}$ describe the edges connecting nodes $\mathbf{P}_4$ and $\mathbf{P}_3$ and nodes $\mathbf{P}_1$ and $\mathbf{P}_2$, respectively. Similarly, the parametric curves $\{\mathbf{D}_l\}_{l=1,2}$ describe the edges connecting nodes $\mathbf{P}_2$ and $\mathbf{P}_3$ and nodes $\mathbf{P}_1$ and $\mathbf{P}_4$, respectively.

In general, part A of Eq. 2 is the part related to the curves, while part B is inherited from the classic isoparametric formulation.

The parametrization of a curved NEFEM quadrilateral element induced by the mapping of Eq. 2 is illustrated in Fig. 1a.

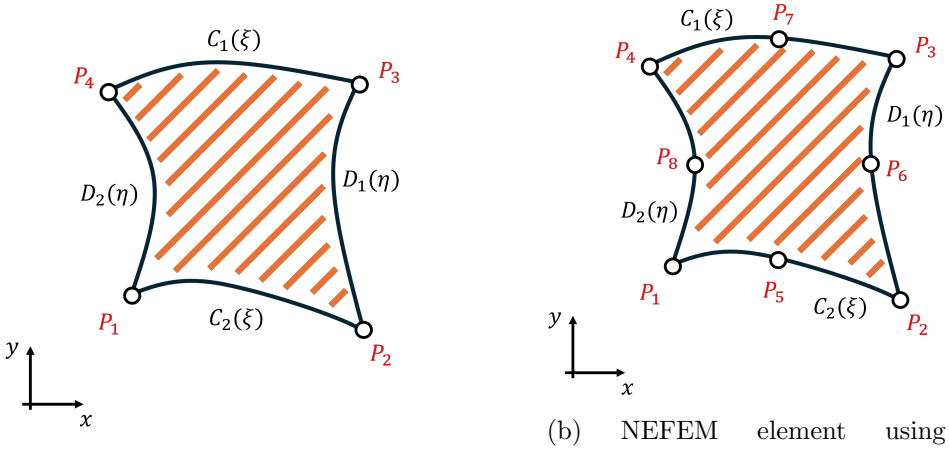

(a) NEFEM element using linear approximation for field solution

(b) NEFEM element using serendipity element for field solution

Figure 1: Comparison between NEFEM $p = 1$ element (a) and NEFEM $p = 2$ element (b)

It is worth noting that for the majority of NEFEM elements, not all the faces are curved, as shown in the latter sections of the paper. When one of the edges of a NEFEM quadrilateral element is straight (i.e. not on the boundary), the parametrization is simply given by the two nodes that connect this edge. For instance, if the edge connecting the nodes $\mathbf{P}_2$ and $\mathbf{P}_3$ is a straight edge, the parametrization $\mathbf{D}_1$ is simply

$$\mathbf{D}_1(\eta) = \eta\,\mathbf{P}_2 + (1-\eta)\,\mathbf{P}_3. \tag{3}$$

In the presented work, Eq. 2 remains unchanged even if the polynomial approximation of the investigated field is higher (here $p = 2$) since the geometrical representation is exact using linear polynomials. This means that if ϕ represents the displacement field, parabolic shape functions will be used according to Eq. 1. On the other hand, if ϕ represents the approximation of the geometry, Eq. 2 will be used where all shape functions N_i are linear. Although the model is not

isoparametric, it allows for the geometric approximation to remain unchanged regardless of the field investigated. The geometry is always exact, regardless of the problem type.

Fig. 1b shows the mapping applied to a parabolic serendipity element which will be used in the following discussion. It can be observed that the serendipity element perfectly matches the element with linear functions, as the mapping is already exact in the first case. The approximation is therefore only improved for the chosen field variable, in this case, the displacements given by elasticity theory.

3 Numerical Results

3.1 Linear Elasticity Model

The considered example is the linear elastic problem, governed by the classical formulation Eq. 4

$$\begin{cases} -\nabla \cdot \boldsymbol{\sigma} = \mathbf{f} & \text{in } \Omega, \\ \mathbf{u} = \mathbf{u}_D & \text{on } \Gamma_D, \\ \mathbf{n} \cdot \boldsymbol{\sigma} = \mathbf{g}_N & \text{on } \Gamma_N, \end{cases} \tag{4}$$

where $\mathbf{u}$ is the displacement field, $\boldsymbol{\sigma}$ is the Cauchy stress tensor, $\mathbf{f}$ denotes a volumetric external force, $\mathbf{u}_D$ is the imposed displacement on the Dirichlet boundary, and $\mathbf{g}_N$ is the imposed traction vector on the Neumann boundary.

The test considered is the so-called Lamé problem. It consists of a thick-walled cylinder of infinite length subject to a uniform internal and external pressure. The solution is computed in a quarter of the domain using the symmetry of the problem as shown in Fig. 2a.

There are no volumetric forces applied, and the exact solution can be written, in polar coordinates, as

$$u(r) = C_1 r + \frac{C_2}{r}, \tag{5}$$

where

$$C_1 = \frac{\nu - 1}{\nu E} \frac{p_e r_e^2 - p_i r_i^2}{r_e^2 - r_i^2}, \quad C_2 = \frac{\nu + 1}{\nu E} \frac{(p_e - p_i) r_e^2 r_i^2}{r_e^2 - r_i^2}. \tag{6}$$

In the above expressions, $r = \sqrt{x^2 + y^2}$, r_e and r_i are the external and internal radii of the annulus respectively, p_e is the external pressure and p_i the internal pressure, ν and E defines the Poisson's ratio and the Young's modulus.

The displacement field is computed using serendipity elements through the proposed NEFEM approach and the error over it is displayed in Fig. 2b.

Results are also presented for a better visualization in Table 1 where the error over FEM and NEFEM is computed as the percentage relative error (Eq. 7) between numerical approximation and reference value.

$$Err = \frac{|\phi_a - \phi_n|}{\phi_a} \tag{7}$$

ϕ_a represents the analytical value while ϕ_n the numerical one.

The contour plots of the displacement also indicate that NEFEM $p = 2$ offers better solution over the boundaries for elastic problem respect to NEFEM $p = 1$. Even if the continuity is not higher between elements, the approximation on the boundary is smoother (Fig. 3).

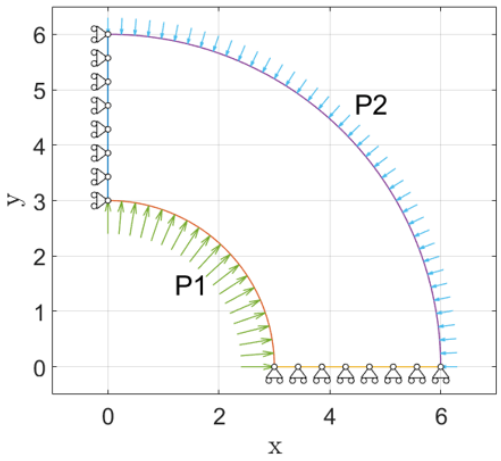

(a) NEFEM element using linear approximation for field solution

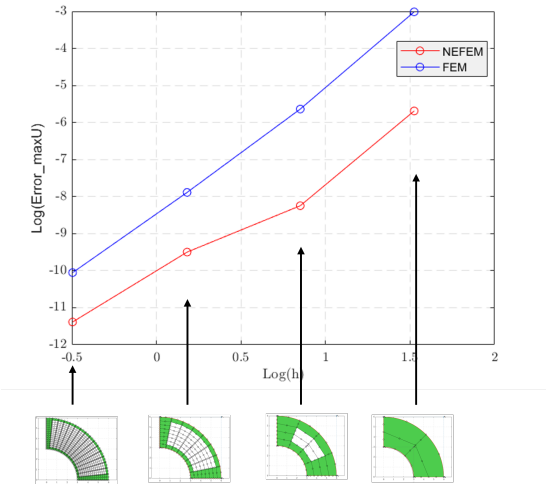

(b) NEFEM element using serendipity element for field solution

Figure 2: Comparison between NEFEM $p = 1$ and NEFEM $p = 2$ elements

	FEM	**NEFEM**	**Err - FEM**	**Err - NEFEM**
4	0.02805	0.029576	4.915254	0.257627
16	0.02940	0.029491	0.355932	0.030508
64	0.029489	0.029498	0.037288	0.006780
256	0.029499	0.029500	0.003390	0.000080
Reference	0.029500			

Table 1: Maximum displacement comparison between FEM and NEFEM.

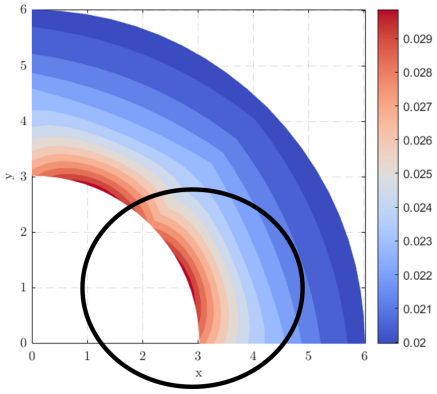

(a) Four NEFEM $p = 1$ elements.

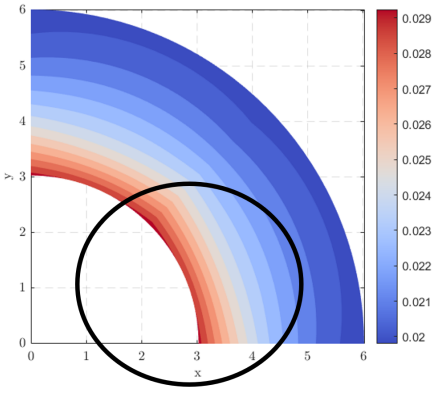

(b) Four NEFEM $p = 2$ elements.

Figure 3: Contour plot displacement of NEFEM elements

3.2 Complex geometries

Having been validated on thick-walled cylinders, the method can be extended to more complex geometries. Specifically, the problem of a flywheel (Fig. 4), which includes challenging geometries and closed loops (holes), has been addressed. The simulation was performed under the application of centrifugal forces. The results indicate that NEFEM elements provide similar displacement outcomes (Fig. 5) compared to traditional serendipity elements in commercial software, but show a significant improvement in terms of total strain energy. It is noteworthy that strain energy calculated as Eq.8 is a unique scalar value for the entire structure giving a good marker of the goodness of the assembled elements.

$$E = \frac{1}{2}\,\mathbf{K}\,\mathbf{U}^2 \tag{8}$$

To achieve the same energy value with FEM it is required approximately 30% more elements as shown in Tab.2.

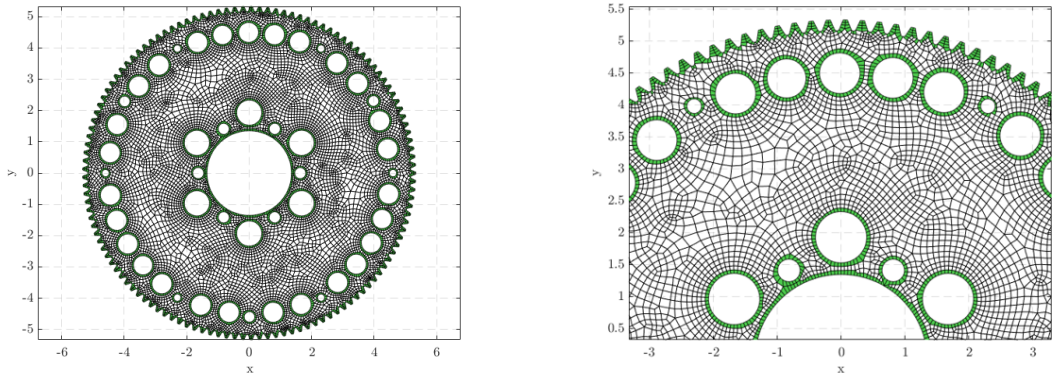

Figure 4: Flywheel mesh using NEFEM $p = 2$ elements.

	NEFEM	**FEM**	**FEM (More Elements)**
No element:	11179	11176	14842
Energy:	0.0059322	0.0059141	**0.005933**

Table 2: Energy value comparison between NEFEM elements and standard Serendipity elements.

Numerous other geometries (Fig. 6), have been tested, further highlighting the flexibility of the method. The ability of NEFEM to accurately handle a wide range of complex shapes, including those with intricate features and varying boundary conditions, demonstrates its robustness and adaptability across different engineering applications. These tests underscore the method's capacity to provide reliable results without the need for extensive manual preprocessing, making it a versatile tool for advanced simulations.

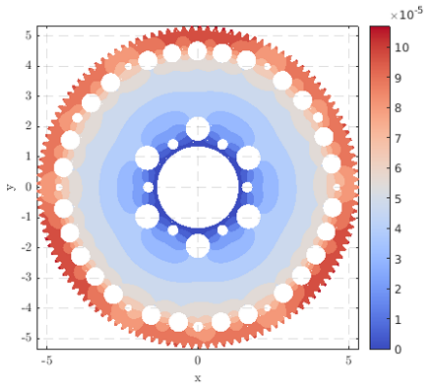

(a) Displacement field using NEFEM $p = 2$.

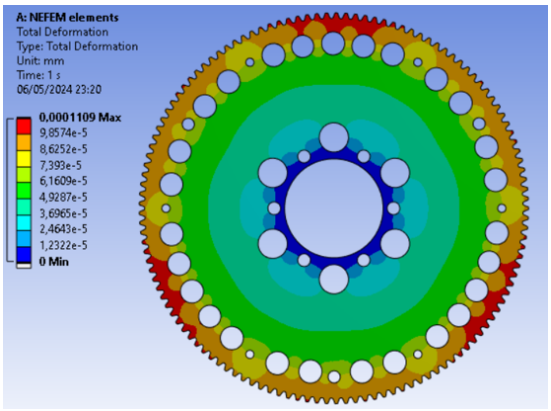

(b) Displacement field using commercial software.

Figure 5: Flywheel displacement field.

4 Conclusion

The primary advantage of NEFEM with a polynomial degree of $p = 2$ lies in its ability to maintain an exact boundary representation throughout the numerical integration process. Unlike traditional FEM, where geometric information can be lost due to approximation, NEFEM ensures that the boundary mapping remains consistent, even when higher-order field approximations are employed. This consistent mapping allows the quadrature process to follow the same rule as in standard FEM, making the method both accurate and computationally efficient.

Moreover, the direct integration of NEFEM with CAD systems, using the boundary representation (B-rep) without any need for conversion to a volumetric representation, distinguishes it from both traditional FEM and isogeometric analysis (IGA). Unlike IGA, which requires a complex transformation from B-rep to V-rep, or standard FEM, which may lose geometric details during mesh generation, NEFEM preserves the exact geometry provided by the CAD model, ensuring that no information is lost.

The introduction of NEFEM to quadrilateral elements and its application to solid mechanics problems within a continuous Galerkin formulation represents a significant advancement for the finite element community. The results from this study demonstrate that NEFEM with $p = 2$ not only matches but often surpasses the accuracy of traditional FEM, especially in scenarios requiring high geometric fidelity. The method's robustness and strong integration with CAD systems make it an ideal choice for complex engineering simulations, where maintaining geometric accuracy is crucial for achieving reliable results.

As NEFEM continues to be refined, its applicability can be expanded to other types of interpolation functions, such as Hermitian or bicubic functions, further broadening its utility in advanced engineering contexts. The flexibility and precision offered by NEFEM, combined with its seamless CAD integration, position it as a powerful tool for future developments in structural mechanics and fluid dynamics.

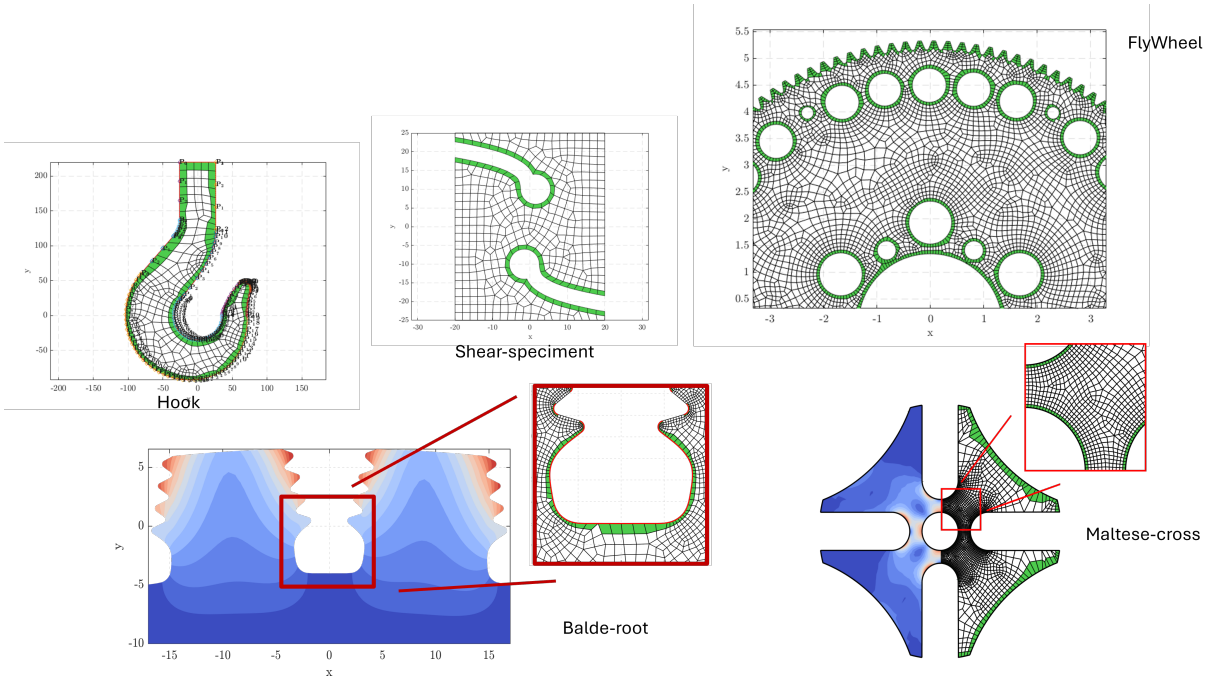

Figure 6: Caption of Figure 2 from the document.

REFERENCES

[1] R. Sevilla, S. Fernández-Méndez, and A. Huerta, "3D NURBS-Enhanced Finite Element Method (NEFEM)," *Internat. J. Numer. Methods Engrg.*, vol. 88, no. 2, pp. 103-125, 2011.

[2] R. Sevilla, S. Fernández-Méndez, and A. Huerta, "NURBS-enhanced finite element method for Euler equations," *Internat. J. Numer. Methods Fluids*, vol. 57, no. 9, pp. 1051-1069, 2008.

[3] R. Sevilla and A. Huerta, "HDG-NEFEM with degree adaptivity for Stokes flows," *J. Sci. Comput.*, vol. 77, no. 3, pp. 1953-1980, 2018.

[4] T.J.R. Hughes, J.A. Cottrell, and Y. Bazilevs, "Isogeometric analysis: CAD, finite elements, NURBS, exact geometry and mesh refinement," *Comput. Methods Appl. Mech. Engrg.*, vol. 194, no. 39-41, pp. 4135-4195, 2005.

[5] K.A. Johannessen, T. Kvamsdal, and T. Dokken, "Isogeometric analysis using LR B-splines," *Comput. Methods Appl. Mech. Engrg.*, vol. 269, pp. 471-514, 2014.

[6] A. Perduta and R. Putanowicz, "Tools and techniques for building models for isogeometric analysis," *Adv. Eng. Softw.*, vol. 127, pp. 70-81, 2019.

[7] P. Ferretti, E. Fusari, G. Alessandri, M. Freddi, and D. Francia, "Stress-Based Lattice Structure Design for a Motorbike Application," *F1000Research*, vol. 11, 2022.

[8] K.J. Bathe, *Finite Element Procedures*, Klaus-Jurgen Bathe, Boston, Mass., 2007.

[9] O.C. Zienkiewicz, R.L. Taylor, and J.Z. Zhu, *The Finite Element Method: Its Basis and Fundamentals*, Sixth Edition, Butterworth-Heinemann, 2005.

[10] M. Montanari, G.M. Santi, R. Sevilla, L. Alfredo, and N. Petrinic, "NURBS-enhanced finite element method (NEFEM) on quadrilateral meshes," *Finite Elements in Analysis and Design*, vol. 231, 2024, Art. no. 104099. doi: 10.1016/j.finel.2023.104099.

[11] S.A. Coons, "Surfaces for Computer-Aided Design of Space Forms," Technical Report, Massachusetts Institute of Technology, USA, 1967.